Published in final edited form as:
Acta Biomater. 2010 November ; 6(11): 4396–4404. doi:10.1016/j.actbio.2010.06.011.

Pyrrole-hyaluronic acid conjugates for decreasing cell binding to metals and conducting polymers

Jae Young Lee[1] and **Christine E. Schmidt**[1,2,3,4,*]

[1]Department of Chemical Engineering, The University of Texas at Austin, Austin, TX

[2]Department of Biomedical Engineering, The University of Texas at Austin, Austin, Texas

[3]Texas Materials Institute, The University of Texas at Austin, Austin, TX

[4]Center for Nano-and Molecular Science and Technology, The University of Texas at Austin, Austin, TX

Abstract

Surface modification of electrically conductive biomaterials has been studied to improve biocompatibility for a number of applications, such as implantable sensors and microelectrode arrays. In this study, we electrochemically coated electrodes with biocompatible and non-cell adhesive hyaluronic acid (HA) to reduce cellular adhesion for potential use in neural prostheses. To this end, pyrrole-conjugated hyaluronic acid (PyHA) was synthesized and employed for electrochemical coating of platinum, indium-tin-oxide, and polystyrene sulfonate-doped polypyrrole electrodes. This PyHA conjugate consists of (1) a pyrrole moiety that allows the compound to be electrochemically deposited onto a conductive substrate and (2) non-adhesive HA to minimize cell adhesion and to potentially decrease inflammatory tissue responses. Our characterization results showed the presence of a hydrophilic p(PyHA) layer on the modified electrode, and impedance measurements revealed impedance that was statistically the same as the unmodified electrode. We found that the p(PyHA)-coated electrodes minimized adhesion and migration of fibroblasts and astrocytes for a minimum of up to 3 months. Also, the coating was stable in physiological solution for 3 months and also stable against enzymatic degradation by hyaluronidase. These studies suggest that this p(PyHA)-coating has the potential to be used to mask conducting electrodes from adverse glial responses that occur upon implantation. In addition, electrochemical coating with PyHA can be potentially extended for the surface modification of other metallic and conducting substances such as stents and biosensors.

Keywords

pyrrole; surface modification; hyaluronic acid; conducting materials

1. Introduction

Biocompatibility of materials is critical for a variety of biomedical applications, such as artificial organs and sensors. In particular, conducting materials have been common choices

*Correspondence to: Christine E. Schmidt, University of Texas at Austin, 1 University Station C0800, Austin, TX 78712, USA, Phone: 1-512-471-1690, Fax: 1-512-471-7060, schmidt@che.utexas.edu.

as implantable materials because of their novel electrical properties and/or good mechanical strength for many biomedical uses such as implantable biosensors, orthopedic implants, and neural prostheses [1-3]. Conducting materials include metals, metal alloys, and conducting polymers (e.g., polypyrrole (PPy)). However, conducting implants often suffer from adverse biological reactions in host tissues, such as the adsorption of proteins onto the implants, biofouling, erosion and release of metallic components, undesirable cell adhesion/activation, and eventual fibrotic scarring [4-7]. These reactions result in inflammatory responses and finally impair the function of the implanted devices. For example, implanted neural electrodes often lose performance within a few months and become unable to record neural signals due to impaired sensitivity and high impedance between the implanted electrode and neural tissues [7,8]. Histological studies have revealed that glial cells (e.g., microglia and astrocytes) are recruited and activated, and form glial scar tissue in the vicinity of the implanted electrodes. Thick glial scar tissue physically and electrically insulates the probes from neurons, which has been proposed as the underlying reason for the loss in their electrical performance of the implanted electrodes [7,9]. Consequently, it is desired to develop biocompatible conducting electrodes that can minimize adverse tissue responses and thus to ensure quality and reliability of the implanted devices.

In particular, hyaluronic acid (HA) is an attractive candidate for surface modification strategies because of its biocompatibility and its general resistance to most cell adhesion [10-14]. HA is a major ECM component that consists of glucuronic acid and N-acetylglucosamine as a repeating disaccharide unit and is present ubiquitously in the body. This polyanionic polysaccharide is non-immunogenic, biocompatible, hydrophilic, and resistant to most cell and plasma protein adhesion [13-15]. Because of these beneficial properties, HA is used for a number of clinical applications including dermal fillers, postoperative peritoneal films preventing tissue adhesions, and coating substances to improve biocompatibility [13,15,16]. For example, stents coated with HA by plasma treatment prevented fibroblast adhesion and reduced platelet deposition and thrombosis [17,18]. Harris et al. grafted anodized titanium surfaces with HA and found no attachment of fibroblasts and osteoblasts on the HA-coated substrates [12]. Also, abdominal surgery using HA-coated polyester meshes showed significantly lower postsurgical adhesion compared to unmodified meshes after two-months [19]. Conventional surface modification methods have been used to modify materials with HA. However, these methods have been developed and explored mostly to immobilize HA on non-conducting surfaces, such as ceramics and synthetic polymers. These conventional methods include adsorption [20], ionic complexation [20,21], and chemical reaction between HA and the underlying material [17,18,22]. Adsorption and ionic complexation rely on non-covalent interactions, such as hydrogen bonding and charge interaction between HA and the underlying substrates. Although covalent links between HA and the material surfaces are stable and desirable, creating strong chemical bonds between HA and substrates requires functionalities that are not always available on biomaterials, especially conductive materials, thus requiring additional activation processes such as plasma treatment and use of a silane coupling reagent [17,22,23]. These techniques also require expensive equipment or toxic coupling reagents. Thus, a simple and effective technique is still desired for HA-immobilization on conducting materials.

In the present study, we electrochemically immobilized electrode surfaces with the biocompatible and non-cell adhesive polysaccharide, HA, and characterized the coating to evaluate suitability for neural electrodes. Specifically, we synthesized a pyrrole-HA conjugate (PyHA) containing a pyrrole moiety that can be oxidized electrochemically under mild conditions to form a stable layer on an electrode surface [2,24,25]. We employed this electrochemically-polymerizable HA for surface modification of platinum (Pt), indium-tin-oxide (ITO), and polystyrene sulfonate-doped polypyrrole (PPyPSS). The PyHA conjugate has electroactive pyrrole moieties capable of interfacing HA with conductive surfaces. We

characterized p(PyHA)-deposited electrodes using multiple techniques including water contact angle measurement, X-ray photoelectron spectroscopy, atomic force microscopy, immunostaining using HA binding protein, and electrochemical impedance spectroscopy. Cortical astrocytes and fibroblasts were cultured in vitro on the p(PyHA)-coated electrodes to study cellular interactions in terms of adhesion and migration. We also investigated the enzymatic stability of the coating and evaluated long-term astrocyte interactions for potential biomedical applications, such as neural prostheses.

2. Materials and Methods

2.1 Materials

All chemicals, cell culture supplements, and disposable tissue culture supplies were purchased from Sigma, Hyclone, and BD, respectively, unless otherwise noted.

2.2 Synthesis of PyHA and p(PyHA)-coated electrodes

2.2.1 Synthesis of pyrrole-HA conjugate—First, 1-aminopropyl pyrrole was synthesized as previously described [26]. In brief, 0.041 mol of 1-(2-cyanoethyl)pyrrole (Sigma) in 300 mL of 0.1 mol $LiAlH_4$ (Aldrich) diethyl ether (Fisher) was refluxed overnight, followed by addition of 3.4 mL of double de-ionized (ddI) water, 7 mL of 20% NaOH, and 3.4 mL of ddI water. The solution was filtered and dried in a vacuum oven for 2 days. A yellow oily product was obtained and stored under N_2 at -20°C. ^{1}H NMR (400 MHz, $CDCl_3$, δ): 1.85 (m, 2H, C**H**$_2$-2), 2.67 (t, 2H, C**H**$_2$-1), 3.95 (t, 2H, 3.95, C**H**$_2$-3), 6.13 (d, 2H, C**H**-α-pyrrole), 6.62 (d, 2H, C**H**-β-pyrrole).

To synthesize pyrrole-HA conjugates (PyHA), 200 mg of HA (1.6×10^6 Da, Fluka) was dissolved in 200 mL ddI water overnight. 198 mg of 1-ethyl-[3-(dimethylamino)propyl]-3-ethyl-carbodiimide (EDC, Sigma) and 116 mg of N-hydroxysuccinimide (NHS, Sigma) were added to the solution. 0.15 mL of 1-aminopropyl pyrrole was added and the pH of the solution was adjusted to 5.5 using 0.2 M HCl (Fisher). After 20 h in reaction, the solution was dialyzed (10,000 Da molecular weight cut-off, Spectrum Laboratories) in ddI water at room temperature for 3 days, exchanging the water every day. The solution was freeze-dried and stored at -20° C. PyHA was characterized using ^{1}H NMR and FT-IR. ^{1}H NMR (400 MHz, D_2O, δ): 1.98 (s, 3H, C(=O)C**H**$_3$), 6.11 (d, 2H, C**H**-α-pyrrole), 6.66 (d, 2H, C**H**-β-pyrrole). The degree of pyrrole addition was calculated based on ^{1}H-NMR from the ratio of the relative peak integrations of the pyrrole protons (peaks at δ 6.1~6.7) and HA's methyl protons (at δ ~1.9). IR spectra of PyHA showed the peaks at 1550 (C=C in pyrrole rings), 1630 (amide I), and 2881 cm^{-1} (aliphatic C-H).

2.2.2 Electrochemical deposition of p(PyHA)—PyHA was electrochemically deposited on a platinum (Pt) slide, an ITO glass slide (sheet resistivity = 30-60 Ω $square^{-1}$, Delta Technologies), or polystyrene sulfonate-doped polypyrrole (PPyPSS) film. ITO slides were used as received. Pt slides were prepared by sputter coating Pt onto plastic polystyrene slides (Ted Pella Inc). The slides were first cleaned by soaking in 20 wt% HNO_3 solution (Fisher) for 30 min, followed by washing with ddI water and a final wash with ethanol. Pt was sputter coated at 30 nm thickness onto the clean slides using a sputter coater (Cressington Scientific Instruments). PPyPSS films were synthesized electrochemically on ITO slides by applying a constant potential of 0.8 V, vs a standard calomel electrode (Fisher), for 5 min in an aqueous solution containing 0.1 M pyrrole (Aldrich) and 0.1 M PSS (Sigma). A computer-assisted potentiostat (Electrochemical Analyzer, CH Instrument) was employed with a three-electrode configuration using a Pt mesh as a counter electrode and a SCE reference electrode. Electrochemical polymerization of PyHA was performed in 5 mg mL^{-1} of PyHA solution in dI water on a conducting substrate in an analogous configuration for PPyPSS synthesis. PyHA

could also serve as a dopant during electrochemical polymerization. For our PyHA conjugates, NMR analysis indicated that the degree of pyrrole substitution was 5-15% on the carboxylic groups of the HA, leaving 85-95% of the carboxylic groups unsubstituted. Thus, PyHA conjugates are negatively charged at physiological conditions and likely serve as dopants as reported previously [27,28], as HA is a polyanionic electrolyte that has been doped during PPy polymerization. A conducting slide (e.g., ITO, Pt, PPyPSS) served as a working electrode. A counter electrode and a reference electrode were a Pt mesh and SCE, respectively. Potential cycling between 0 and 1.0 V, versus a SCE, was employed at a scan rate of 0.1 V s^{-1}. Twenty cycles were applied for each substrate. For comparison, unmodified HA solution was also prepared and treated under the same conditions. After deposition, the samples were washed extensively with ddI water, dried in a vacuum oven overnight, and stored in a desiccator.

2.3 Characterization of p(PyHA)-coated conducting substrates

2.3.1 Water contact angle measurement—Static water contact angles were measured using a goniometer (Edmund Optics) assembled with a Navitar CV-M30 camera to study the wettability of the native electrodes and the p(PyHA)-coated electrodes. A 2 μL drop of ultrapure water was placed on the surface of the samples at room temperature. Average angles were collected from at least three different samples.

2.3.2 X-ray photon spectroscopy (XPS)—XPS analysis using a Kratos AXIS Ultra XPS system was performed to study surface elemental compositions. The system was operated at 1×10^{-9} Torr chamber pressure, 15 kV and 150 W Al X-ray source. High-resolution spectra were collected with 20 eV pass energy at takeoff angles of 90° between the sample and analyzer. Calibration of the binding energy was performed by setting *C*-C/*C*–H component in C_{1s} peak at 284.7 eV. Peaks were deconvoluted using XPSPEAK software to characterize each atom.

2.3.3 Atomic force microscopy (AFM)—Dry samples were analyzed with AFM (MFP 3D, Asylum Research) to assess surface topography and thickness of the coated p(PyHA) layer. AFM was operated in a contact mode using silicon nitride probes (Veeco) at a scan rate of 0.2 Hz. Images were analyzed using Igor Pro MFP-3D software (Asylum Research). Root mean square (RMS) roughness was calculated from 512 × 512 scans of 10 × 10 μm section of the sample. Thickness of the coating was calculated from the scanned images at a border of the bare area and the p(PyHA)-coated area.

2.3.4 Electrochemical impedance spectroscopy (EIS)—Electrochemical impedance spectra of p(PyHA)-coated electrodes were measured and compared with unmodified electrodes using an electrochemical impedance spectroscope (Electrochemical Analyzer, CH Instruments). For EIS analysis, polydimethylsiloxane (PDMS, Dow-Corning) well was attached to the electrode surface. The electrodes were electrochemically coated with PyHA and washed thoroughly with ddI water as described above. A three-electrode cell was employed, consisting of a sample electrode as a working electrode, a Pt mesh counter electrode, and SCE reference electrode. Impedance spectra of three samples for each condition were collected in a range of $1\text{-}10^5$ Hz, applying an AC sinusoidal signal with 10 mV in 50 mM PBS (pH 7.2).

2.4 Cell culture

Normal human dermal fibroblasts (nHDF, Lonza) were maintained in T-75 tissue culture flasks (Corning) with 5% CO_2 at 37°C in Dulbecco's modified Eagle's medium (DMEM, Hyclone) containing 10% fetal bovine serum (Hyclone) and passaged every week. Astrocytes were isolated from cerebral cortices of 2-day old Sprague-Dawley rats (Charles River), as previously described [29]. Briefly, the cerebral cortices were finely chopped and digested with trypsin/EDTA solution (Sigma) at 37°C for 30 min, followed by mechanical trituration using a Pasteur

pipette. After centrifugation (500 g, 10 min), cells were resuspended in culture medium consisting of DMEM, 10% fetal bovine serum, and 1% penicillin streptomycin antibiotic solution (Sigma), and then plated in a poly-L-lysine (Sigma) coated T-75 flask with a density of 10^6 cells per cm^2. After 7 days of incubation, the flask was vigorously shaken on an orbital shaker at 280 rpm overnight to remove loosely-bound cells (i.e., oligodendrocytes and microglia cells); attached astrocytes were then removed using trypsin/EDTA and replated onto a poly-L-lysine coated plate. The purity of the astrocytes was assessed by immunostaining using an antibody for glial fibrillary acidic protein (GFAP), which is only expressed by astrocytes; > 95% of cells were GFAP positive. Astrocytes were maintained in DMEM/F12-K medium (Sigma) supplemented with 10% fetal bovine serum on poly-L-lysine coated tissue culture plates with 5% CO_2 at 37°C. Cells were fed every other day and passaged every week. For adhesion studies, PDMS wells (1 cm × 1 cm inner dimension) were placed on bare substrates and p(PyHA)-coated substrates, followed by UV sterilization (30 min). Cells were seeded at a density of 3×10^4 cells per cm^2 into each well and incubated. For long-term culture on p(PyHA)-patterned substrates, PDMS wells (1 cm × 1 cm inner dimension) were placed on p(PyHA)-patterned substrates (circular pattern, 3 mm diameter) slides. Cells were seeded at a density of 1×10^4 cells per cm^2 on each substrate. Cells were fed every other day.

To demonstrate the role of HA in preventing cell adhesion, p(PyHA)-coated substrates were exposed to a very high concentration of HAase solution (500 U mL^{-1}) in PBS (pH 7.2) at 37° C for 24 h to completely degrade the immobilized-HA. In addition, to study long-term interactions between the coating and astrocytes, cells were cultured on the p(PyHA)-coated Pt and ITO electrodes for 1 month and 3 months, respectively. During culture, cell adhesion and migration was monitored at the border between HA-coated area and unmodified area.

2.5 Immunofluorescence and image analysis

After culture, cells were fixed with 4% paraformaldehyde (Sigma) in PBS buffer for 30 min and incubated in a permeabilizing and blocking solution (0.1% Triton X-100 (Fluka), 3% goat serum (Sigma) in PBS) for 60 min. The nHDF cells were stained with Alexa Fluor 488-labeled phalloidin (Invitrogen) for 30 min for actin filaments and with 4',6-diamidino-2-phenylindole dilactate (DAPI, Invitrogen) for nuclei, washed with PBS buffer twice, and stored at 4°C until analysis. For astrocyte staining, the cells were immunestained with mouse anti-GFAP antibody (1:200 dilution) (Sigma) at 4°C overnight and washed with PBS buffer three times (5 min each), followed by treatment with Alexa Fluor 488-labeled goat anti-mouse antibody (1:500) (Molecular Probes). Nuclei were stained with DAPI (1:1000 dilution) at room temperature for 5 min. For HA staining, the substrates were incubated in PBS containing biotinylated-HABP (bHABP, 1:200) (Calbiochem) for 1 h, washed with PBS two times, treated with streptavidin-PE (1:500) (Molecular Probes) in PBS for 1 h, and washed with PBS three times.

Immunofluorescence and phase contrast images were acquired using a fluorescence microscope (IX-70, Olympus) equipped with a color CCD camera (Optronics MagnaFire). The cell images were processed using Adobe Photoshop and Image J (NIH) software. Numbers of nuclei on the substrates were measured from five random images and reported.

2.6 Stability tests

Stability of the p(PyHA)-coated electrodes was explored by incubating the modified electrodes in either PBS or PBS with hyaluronidase, and then assessing the ability of the incubated p (PyHA) layer to prevent cell adhesion and migration. For the former study, sterile p(PyHA)-coated ITO electrodes were incubated in PBS at 37°C for 3 months. Then, astrocytes were seeded onto the incubated electrodes and cultured for 3 days. For the enzymatic stability test, the p(PyHA)-coated substrates were incubated in solutions of various HAase activities (5×10^{-4}, 5×10^{-3}, 5×10^{-2}, 5×10^{-1}, 5, 50, and 500 U mL^{-1} in PBS) at 37°C for 24 h and used for

subsequent water contact angle measurement, immunostaining for HA using bHABP and streptavidin-PE, and in vitro astrocyte culture.

3. Results

3.1 Synthesis and electrochemical polymerization of pyrrole-HA conjugate (PyHA)

To produce a functionalized pyrrole that can be conjugated with HA, we first synthesized 1-aminopropyl pyrrole from 2-cyanoethyl pyrrole by reduction using $LiAlH_4$ in diethyl ether. Then, PyHA was synthesized by coupling 1-aminopropyl pyrrole to carboxylic groups on HA via EDC/NHS chemistry (Fig. 1). Analysis by ^1H NMR indicated approximately 5-15 % substitution of pyrrole units on the carboxylic groups of HA. Thus, this synthesized PyHA consists of (1) a pyrrole moiety that allows the compound to be electrochemically deposited onto a conductive substrate and (2) non-adhesive HA to minimize cell adhesion and to potentially decrease glial scar formation.

The PyHA conjugate was electrochemically polymerized onto conducting substrates using potentiodynamic electropolymerization. Twenty cycles of linear sweeping potentials from 0 to 1.0 V versus SCE were applied in a PyHA solution at a scan rate of 0.1 V s^{-1}. We also repeated the same electrochemical procedure using unmodified HA solution, not PyHA, to determine whether there was any possible electrochemical oxidation of HA without the intermediate pyrrole moiety. No significant oxidation was observed in HA solution, whereas oxidation of PyHA is observed above 0.8 V (Fig. 2), suggesting that HA deposition was achieved only through oxidation of pyrrole moieties. In addition to metallic electrodes, a stable HA-coating was applied to a non-metallic conductive electrode of PPyPSS.

3.2 Surface characterization of p(PyHA)-coated electrodes

The surface characteristics of PyHA-deposited electrodes were characterized to assess suitability of these materials for biomedical applications including neural prosthetic probes. Electrochemically-coated p(PyHA) was confirmed by immunostaining using bHABP and streptavidin tagged with phycoerythrin (streptavidin-PE). Bright fluorescence was observed on the HA-coated electrodes of ITO and Pt, whereas no detectable fluorescence was observed for the bare electrodes treated with the same staining and imaging conditions as the p(PyHA)-coated substrates.

Water contact angle measurement showed that the wettability of p(PyHA)-coated ITO (27.9 ±1.5°) and p(PyHA)-coated Pt (31.5±2.1°) was greatly improved compared to the bare ITO (87.8±1.1°) and the bare Pt (81.4±1.6°); this result illustrates an increase in the hydrophilicity of the electrode surface with the addition of the hydrophilic HA-based coating. This dramatic decrease in water contact angles after p(PyHA) coating is consistent with other research for immobilization of HA or HA-derivatives on surfaces [22,30].

Surface chemical elements of the samples were analyzed using X-ray photon spectroscopy (XPS). As shown in Fig. 3, peaks at 284.7 eV (C-C/C-H), 286.3 eV (C-N/C-O), and 288.3 eV (O=C-O) were observed after p(PyHA) deposition on the ITO slide; these peaks were found in the HA spectra as published by other groups [20,22,23]. A new nitrogen peak at 400.1 eV, attributable to pyrrole nitrogen (C-N) and amide bonds in the PyHA, was also detected after coating p(PyHA) on the ITO. Similar spectra and peaks were observed from p(PyHA)-coated Pt slides (data not shown). This spectroscopic analysis demonstrated the presence of HA on the electrode surface.

Atomic force microscopy (AFM) was employed to assess surface topographies of dry substrates. Fig. 4 shows distinct changes in surface topography after electrochemical PyHA polymerization, which also further confirms the presence of the p(PyHA) coating. The p

(PyHA)-coated Pt electrode showed lower root-mean-square roughness of 2.49 nm compared to the bare Pt electrode (3.05 nm). Interestingly, fine aggregates of approximately 10 nm were found over the p(PyHA)-coated Pt substrates. These nano-sized aggregates may result from HA clustering during drying, which has been observed on variously prepared HA-immobilized materials by other groups [20,31,32]. We also measured the coating thickness by scanning borders between the HA-coated area and the uncoated area of the sample. A p(PyHA) layer of approximately 20 – 40 nm thickness was calculated from AFM micrographs.

Electrical impedance of the modified electrode was also evaluated as one of the critical parameters, because possible loss of electrical sensitivity (e.g., increase in impedance) may be a concern when modifying neural electrodes or biosensors [24,33]. As shown in Fig. 5, the electrochemical impedance spectra of p(PyHA)-coated Pt show no significant differences from those of bare Pt, respectively, across a range of frequencies (10^0-10^5 Hz) including 1 kHz which is relevant to neural probes [24,33]. We also performed EIS measurements for p(PyHA)-coated ITO, which displayed no significant changes in impedance compared to unmodified ITO.

3.3 In vitro cell culture on the p(PyHA)-coated substrates

Cellular interactions with the HA-coated electrodes were explored with in vitro culture of fibroblasts and cortical astrocytes. As shown in Fig. 6, no fibroblasts or astrocytes attached to the HA-coated ITO, whereas most cells were found to adhere and grow well on the uncoated ITO, indicating that the p(PyHA)-coating is non-cell adhesive. Immunostaining clearly illustrates that astrocytes did not adhere to or move onto the area stained for HA, suggesting that the immobilized-HA plays a direct role in preventing astrocyte adhesion. Furthermore, complete enzymatic removal of HA using a high concentration of hyaluronidase (HAase) permitted astrocyte adhesion and growth, and resulted in a confluent layer of cells similar to cells grown on the bare ITO electrode (Fig. 6B). For this study, we used an activity of HAase (500 U mL^{-1}) higher than tissue activity (e.g., ~2.8 U mL^{-1} in human serum [34]) to ensure complete degradation of the immobilized-HA.

Additionally, the effectiveness of the p(PyHA) coating on different conducting materials, such as Pt and PPyPSS, was studied by performing in vitro astrocyte culture. Electrochemical deposition of p(PyHA) on the Pt and PPyPSS substrates prohibited cellular growth; however, astrocytes grew very well on all unmodified substrates (Fig. 7). These results suggest that the p(PyHA)-coating can be generally applicable for modification of a number of different conducting materials to create non-cell adhesive surfaces for biomedical applications that require conducting substrates but minimized cellular interactions.

3.4. Stability tests of the p(PyHA) coatings

We performed stability tests for the p(PyHA)-coated electrodes. To study stability of the p (PyHA) coatings in a physiological condition, we incubated the p(PyHA)-coated ITO substrates in phosphate-buffered saline (PBS) at 37°C for 3 months. Astrocytes were then cultured on the incubated substrates to monitor cell adhesion and migration. As shown in Fig. 8A, the substrates did not allow astrocytes to attach to or migrate onto the HA-coated area. Also, the p(PyHA)-coating was substantially stained by bHABP. These results indicate that the HA-coating is functionally stable under physiological conditions. Long-term cell culture was also performed to study prolonged interactions between astrocytes and the p(PyHA) coating. Astrocytes were cultured on the p(PyHA)-coated Pt for 1 month; immunostaining showed that the immobilized-HA was present and effective in minimizing astrocyte adhesion and migration (Fig. 8B). Moreover, we monitored astrocytes for 3 months at the border between the HA-patterned area and bare ITO (Fig. 8C). The astrocytes did not migrate to the HA-patterned area on ITO even after 3 months (90 days). Astrocytes grew to confluence by day 10 in culture on the unmodified ITO area, but not on the p(PyHA)-patterned area. These results

indicate that the electrochemically deposited p(PyHA) coatings were functionally stable on conductive materials both under physiological conditions and in the presence of cells. Importantly, growth of astrocytes cultured on ITO and Pt was found to not be influenced by the presence of immobilized-p(PyHA) next to the cells, suggesting that the p(PyHA)-coated electrode is not cytotoxic to neighboring cells.

The HA coating may be exposed to HAase in vivo. For example, surgical insertion of implants (e.g., neural probes) leads to a temporary disruption of blood vessels [35], possibly resulting in release of serum HAase (~2.6 U mL^{-1} in human serum) [34]. Thus, it is possible that the electrodes' ability to prevent cell attachment and migration in vivo can be impaired. Hence, we incubated the p(PyHA)-coated electrodes in solutions containing various activities of HAase (5×10^{-4}– 500 U mL^{-1} in PBS) for 24 h. Water contact angles and immunofluorescence of the HAase-treated substrates were measured (Fig. 9A and 9B). Astrocytes were also cultured on the HAase-treated electrodes to assess enzymatic stability of the p(PyHA) coatings (Fig. 9C). After 24 h incubation in solutions containing up to 5 U mL^{-1} of HAase, the p(PyHA)-coated electrodes maintained their hydrophilicity, ability to bind to HABP, and ability to prevent astrocyte adhesion. These results suggest negligible HA degradation under these conditions. Since normal HAase is rarely active above pH 4.5 [36] and its expression in brain is essentially negligible [37], we speculate that the p(PyHA)-coated electrode would experience minimal degradation in the brain post implantation.

4. Discussion

In this study, we utilized electrochemical polymerization methods for surface modification of conducting materials with HA. Electrochemical coating procedures in general have various advantages including simple and inexpensive processing, and general applicability to any conductive material [2,24,38]. Importantly, use of the PyHA conjugate for electrochemical coating is substantially different from that of HA-doped polypyrrole, which can be prepared during electrochemical polymerization of pyrrole from a solution of pyrrole monomer and HA [27,39]. In particular, for HA-doped PPy, the HA is not stably integrated into the PPy films, unlike with the PyHA conjugate. Dopant molecules in general have been shown to be released from conducting polymers as a result of de-doping and/or dopant exchange [38,40]. For example, Collier et al. found that the ability of HA-doped films to bind to biotinylated HA binding protein (bHABP) decreased to 30% after one day of incubation in culture medium at 37°C [27]. It was also shown that PC12 cell adhesion on HA-doped PPy films was not different from that on PSS-doped PPy films, suggesting a loss of the HA from the PPy substrate. In another study, adhesion of osteoblasts on HA-doped PPy films was not consistently minimized, but was greatly influenced by electrochemical polymerization conditions [39]. No cells were found on films synthesized at a high current density, whereas cells adhered on the films produced at a low current density [39]. These studies suggest that HA incorporation into PPy films is possible, but is inconsistent and highly dependent on synthesis conditions, and once incorporated, the HA dopant is not stably integrated into the PPy and thus can leach from the polymer films. In contrast, for the pyrrole-HA conjugate used in this present study, pyrrole and HA are covalently linked together so that HA strands are unlikely to be released from the polymer surfaces. Our studies demonstrate a stability for a minimum of 3 months both under physiological conditions and in cell culture conditions.

The p(PyHA)-coated electrodes exhibited hydrophilic surface properties. The p(PyHA)-coated ITO and Pt electrodes showed water contact angles of 27.9±1.5° and 31.5±2.1°, respectively. The p(PyHA)-coated ITO remained hydrophilic (21.6±7.3° water contact angle) even after incubation in solution containing 5 U mL^{-1} HAase. Hydrophilic surfaces are known to reduce non-specific plasma protein adsorption that leads to inflammatory responses [41]. Therefore,

functionalization of hydrophobic electrode surfaces with the hydrophilic HA should improve biocompatibility.

In general, polymeric forms of functionalized pyrrole derivatives decrease conductivities compared to pristine PPy due to hindrance of the structural planarity of π–electron conjugation in the polymeric chains of pyrrole [2,42]. PyHA conjugates used in this study were prepared from N-functionalized pyrrole monomer (i.e., 1-aminopropyl pyrrole). However, we observed no statistical increase in impedances after the electrochemical polymerization of PyHA. We speculate that a nanometer-thick coating of the highly charged polymer, PyHA, might have little influence on charge transfer at interfaces. This finding is consistent with a separate study on enzyme-based biosensors in which electrodes coated with a pyrrole-alginate conjugate showed no negative impact on impedance [43].

5. Conclusion

In this study, we synthesized a PyHA conjugate that was used to electrochemically polymerize a a stable thin HA-coating (20-40 nm in thickness) on conducting substrates (e.g., ITO, Pt, PPyPSS). Immobilized-HA rendered the electrode surfaces hydrophilic and resistant to fibroblast and astrocyte adhesion. The p(PyHA)-coated electrodes also retained electrical properties of the underlying electrode materials. Furthermore, p(PyHA)-coated electrodes were found to be stable under physiological conditions and were able to prevent astrocyte adhesion and migration for three months. In addition, the p(PyHA)-coating was stable at HAase concentrations that are relevant for neural prosthetic applications. Thus, effectiveness of the p (PyHA) coating to minimize astrogliosis should be tested in vivo with commercial neural probes. This approach for surface modification of metallic and non-metallic conducting substances can also be extended for use in other applications such as stents and biosensors.

Acknowledgments

This work was supported by NIH R01EB004429. The authors would like to thank Stephanie Seidlits and Dr. Zin Khaing for isolation of cortical astrocytes, Dr. Jonathan Nickels for help with atomic force microscopy, and Dr. Scott Zawko for proof reading the manuscript.

References

1. Geetha M, Singh AK, Asokamani R, Gogia AK. Ti based biomaterials, the ultimate choice for orthopaedic implants - A review. Prog Mater Sci 2009;54:397.
2. Guimard NK, Gomez N, Schmidt CE. Conducting polymers in biomedical engineering. Progress in Polymer Science 2007;32:876.
3. Ratner, BD. Biomaterials science : an introduction to materials in medicine. Amsterdam; Boston: Elsevier Academic Press; 2004.
4. Wisniewski N, Moussy F, Reichert WM. Characterization of implantable biosensor membrane biofouling. Fresenius J Anal Chem 2000;366:611. [PubMed: 11225773]
5. Uo M, Watari F, Yokoyama A, Matsuno H, Kawasaki T. Tissue reaction around metal implants observed by X-ray scanning analytical microscopy. Biomaterials 2001;22:677. [PubMed: 11246961]
6. Keselowsky BG, Bridges AW, Burns KL, Tate CC, Babensee JE, LaPlaca MC, Garcia AJ. Role of plasma fibronectin in the foreign body response to biomaterials. Biomaterials 2007;28:3626. [PubMed: 17521718]
7. Grill WM, Norman SE, Bellamkonda RV. Implanted Neural Interfaces: Biochallenges and Engineered Solutions. Annu Rev Biomed Eng. 2009
8. Polikov VS, Tresco PA, Reichert WM. Response of brain tissue to chronically implanted neural electrodes. Journal of Neuroscience Methods 2005;148:1. [PubMed: 16198003]

9. Turner JN, Shain W, Szarowski DH, Andersen M, Martins S, Isaacson M, Craighead H. Cerebral astrocyte response to micromachined silicon implants. Experimental Neurology 1999;156:33. [PubMed: 10192775]
10. Morra M, Cassineli C. Non-fouling properties of polysaccharide-coated surfaces. J Biomater Sci Polym Ed 1999;10:1107. [PubMed: 10591135]
11. Volny M, Elam WT, Ratner BD, Turecek F. Enhanced in-vitro blood compatibility of 316L stainless steel surfaces by reactive landing of hyaluronan ions. J Biomed Mater Res B Appl Biomater 2007;80:505. [PubMed: 16838347]
12. Harris LG, Patterson LM, Bacon C, Gwynn I, Richards RG. Assessment of the cytocompatibility of different coated titanium surfaces to fibroblasts and osteoblasts. J Biomed Mater Res A 2005;73:12. [PubMed: 15704113]
13. Morra M. Engineering of biomaterials surfaces by hyaluronan. Biomacromolecules 2005;6:1205. [PubMed: 15877335]
14. Park YD, Tirelli N, Hubbell JA. Photopolymerized hyaluronic acid-based hydrogels and interpenetrating networks. Biomaterials 2003;24:893. [PubMed: 12504509]
15. Lapcik L, Lapcik L, De Smedt S, Demeester J, Chabrecek P. Hyaluronan: Preparation, structure, properties, and applications. Chemical Reviews 1998;98:2663. [PubMed: 11848975]
16. Laurent, TC. The chemistry, biology, and medical applications of hyaluronan and its derivatives. London; Miami: Portland Press; 1998.
17. Pitt WG, Morris RN, Mason ML, Hall MW, Luo Y, Prestwich GD. Attachment of hyaluronan to metallic surfaces. J Biomed Mater Res A 2004;68:95. [PubMed: 14661254]
18. Verheye S, Markou CP, Salame MY, Wan B, King SB 3rd, Robinson KA, Chronos NA, Hanson SR. Reduced thrombus formation by hyaluronic acid coating of endovascular devices. Arterioscler Thromb Vasc Biol 2000;20:1168. [PubMed: 10764689]
19. Lise M, Belluco C, Pucciarelli S, Meggiolaro F, Codello L, Pressato D, Dona M, Bigon E. Prevention of adhesions in abdominal surgery. New Frontiers in Medical Sciences: Redefining Hyaluronan 2000;1196:339.
20. Suh KY, Yang JM, Khademhosseini A, Berry D, Tran TN, Park H, Langer R. Characterization of chemisorbed hyaluronic acid directly immobilized on solid substrates. J Biomed Mater Res B Appl Biomater 2005;72:292. [PubMed: 15486967]
21. Burke SE, Barrett CJ. pH-responsive properties of multilayered poly(L-lysine)/hyaluronic acid surfaces. Biomacromolecules 2003;4:1773. [PubMed: 14606908]
22. Cen L, Neoh KG, Kang ET. Surface functionalization of electrically conductive polypyrrole film with hyaluronic acid. Langmuir 2002;18:8633.
23. Thierry B, Winnik FM, Merhi Y, Griesser HJ, Tabrizian M. Biomimetic hemocompatible coatings through immobilization of hyaluronan derivatives on metal surfaces. Langmuir 2008;24:11834. [PubMed: 18759386]
24. Green RA, Lovell NH, Wallace GG, Poole-Warren LA. Conducting polymers for neural interfaces: challenges in developing an effective long-term implant. Biomaterials 2008;29:3393. [PubMed: 18501423]
25. Ateh DD, Navsaria HA, Vadgama P. Polypyrrole-based conducting polymers and interactions with biological tissues. J R Soc Interface 2006;3:741. [PubMed: 17015302]
26. Rajesh, Bisht V, Takashima W, Kaneto K. An amperometric urea biosensor based on covalent immobilization of urease onto an electrochemically prepared copolymer poly (N-3-aminopropyl pyrrole-co-pyrrole) film. Biomaterials 2005;26:3683. [PubMed: 15744952]
27. Collier JH, Camp JP, Hudson TW, Schmidt CE. Synthesis and characterization of polypyrrole-hyaluronic acid composite biomaterials for tissue engineering applications. J Biomed Mater Res 2000;50:574. [PubMed: 10756316]
28. Gilmore KJ, Kita M, Han Y, Gelmi A, Higgins MJ, Moulton SE, Clark GM, Kapsa R, Wallace GG. Skeletal muscle cell proliferation and differentiation on polypyrrole substrates doped with extracellular matrix components. Biomaterials 2009;30:5292. [PubMed: 19643473]
29. Banker, G.; Goslin, K. Cellular and Molecular Neuroscience Series Culturing Nerve Cells. In: Banker, G.; Goslin, K., editors. Cellular and Molecular Neuroscience Series: Culturing Nerve Cells. Mit Press; Cambridge, Massachusetts, USA; London, England, Uk: 1991. p. XIII-453P.Illus

30. Yoo HS, Lee EA, Yoon JJ, Park TG. Hyaluronic acid modified biodegradable scaffolds for cartilage tissue engineering. Biomaterials 2005;26:1925. [PubMed: 15576166]

31. Ibrahim S, Joddar B, Craps M, Ramamurthi A. A surface-tethered model to assess size-specific effects of hyaluronan (HA) on endothelial cells. Biomaterials 2007;28:825. [PubMed: 17045332]

32. Wang A, Cao T, Tang H, Liang X, Black C, Salley SO, McAllister JP, Auner GW, Ng KY. Immobilization of polysaccharides on a fluorinated silicon surface. Colloids Surf B Biointerfaces 2006;47:57. [PubMed: 16387479]

33. Cui X, Wiler J, Dzaman M, Altschuler RA, Martin DC. In vivo studies of polypyrrole/peptide coated neural probes. Biomaterials 2003;24:777. [PubMed: 12485796]

34. Delpech B, Bertrand P, Chauzy C. An indirect enzymoimmunological assay for hyaluronidase. J Immunol Methods 1987;104:223. [PubMed: 3316396]

35. Boast CA, Reid SA, Johnson P, Zornetzer SF. A caution to brain scientists: unsuspected hemorrhagic vascular damage resulting from mere electrode implantation. Brain Res 1976;103:527. [PubMed: 766914]

36. Margolis RU, Margolis RK, Atherton DM, Santella R. Hyaluronidase of Brain. Journal of Neurochemistry 1972;19:2325. [PubMed: 4658791]

37. Garg, HG.; Hales, CA. Chemistry and biology of hyaluronan. Amsterdam; Boston: Elsevier; 2004.

38. Fonner JM, Forciniti L, Nguyen H, Byrne JD, Kou YF, Syeda-Nawaz J, Schmidt CE. Biocompatibility implications of polypyrrole synthesis techniques. Biomed Mater 2008;3:034124. [PubMed: 18765899]

39. Serra Moreno J, Panero S, Materazzi S, Martinelli A, Sabbieti MG, Agas D, Materazzi G. Polypyrrole-polysaccharide thin films characteristics: electrosynthesis and biological properties. J Biomed Mater Res A 2009;88:832. [PubMed: 18980193]

40. Maddison DS, Jenden CM. Dopant Exchange in Conducting Polypyrrole Films. Polym Int 1992;27:231.

41. Thevenot P, Hu WJ, Tang LP. Surface chemistry influences implant biocompatibility. Current Topics in Medicinal Chemistry 2008;8:270. [PubMed: 18393890]

42. Jung YA, Lee KH, Park CW, Suh TS, Hong CM, Hong SH, Ahn WS, Chun HJ. Characterization of surface-modified poly(DL-lactide-co-glycolide) scaffolds from hydrophilic monomers using plasma-enhanced CVD. Journal of Industrial and Engineering Chemistry 2005;11:165.

43. Abu-Rabeah K, Marks RS. Impedance study of the hybrid molecule alginate-pyrrole: Demonstration as host matrix for the construction of a highly sensitive amperometric glucose biosensor. Sens Actuator B-Chem 2009;136:516.

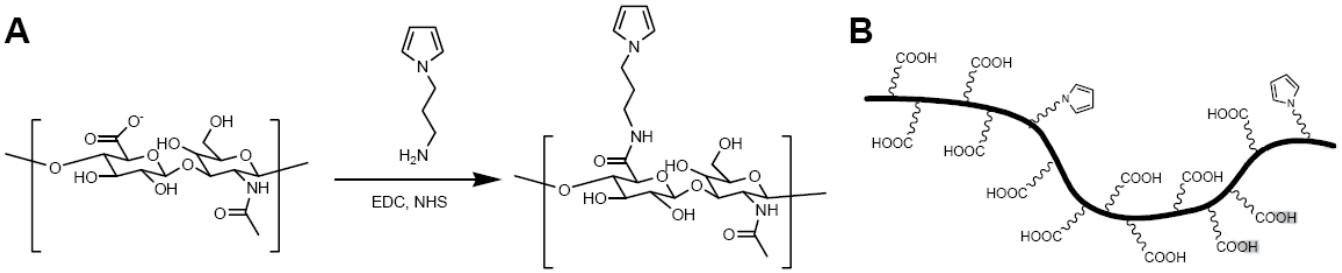

Figure 1.

(A) The chemical structure of the PyHA conjugate synthesis. PyHA conjugate was synthesized by coupling 1-aminopropyl pyrrole to the carboxylic groups of HA. (B) Schematic of the PyHA conjugate illustrating the degree of substitution of the HA with the pyrrole. ^{1}H NMR analysis indicated that approximately 5-15% of carboxylic groups were modified with pyrrole.

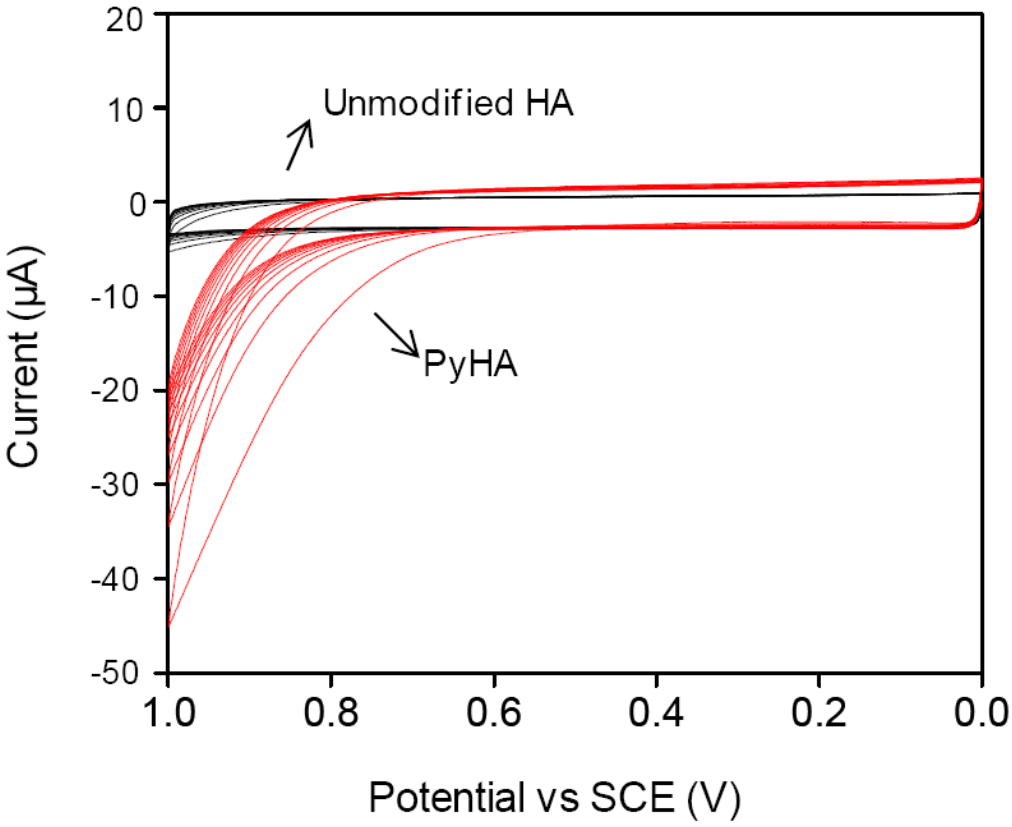

Figure 2.
Voltammogram of the potentiodynamic synthesis with PyHA (red lines) on ITO in 0.5 wt% aqueous polymer solution. Twenty cycles from 0 V to 1.0 V, versus SCE, were applied with a scan rate of 0.1 V s^{-1}. The same electrochemical procedure was repeated using unmodified HA solution (black lines). Electrochemical oxidation was observed above 0.8 V with PyHA, but not with unmodified HA.

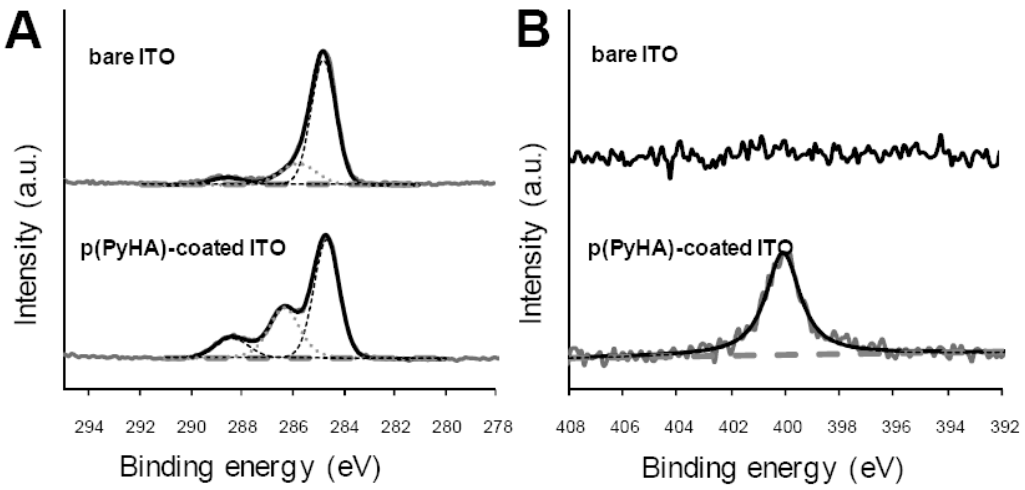

Figure 3.
High resolution (A) C_{1s} and (B) N_{1s} XPS spectra of bare ITO and p(PyHA)-coated ITO. After p(PyHA) coating, distinct changes in spectra were observed, suggesting the presence of the p (PyHA) on surfaces.

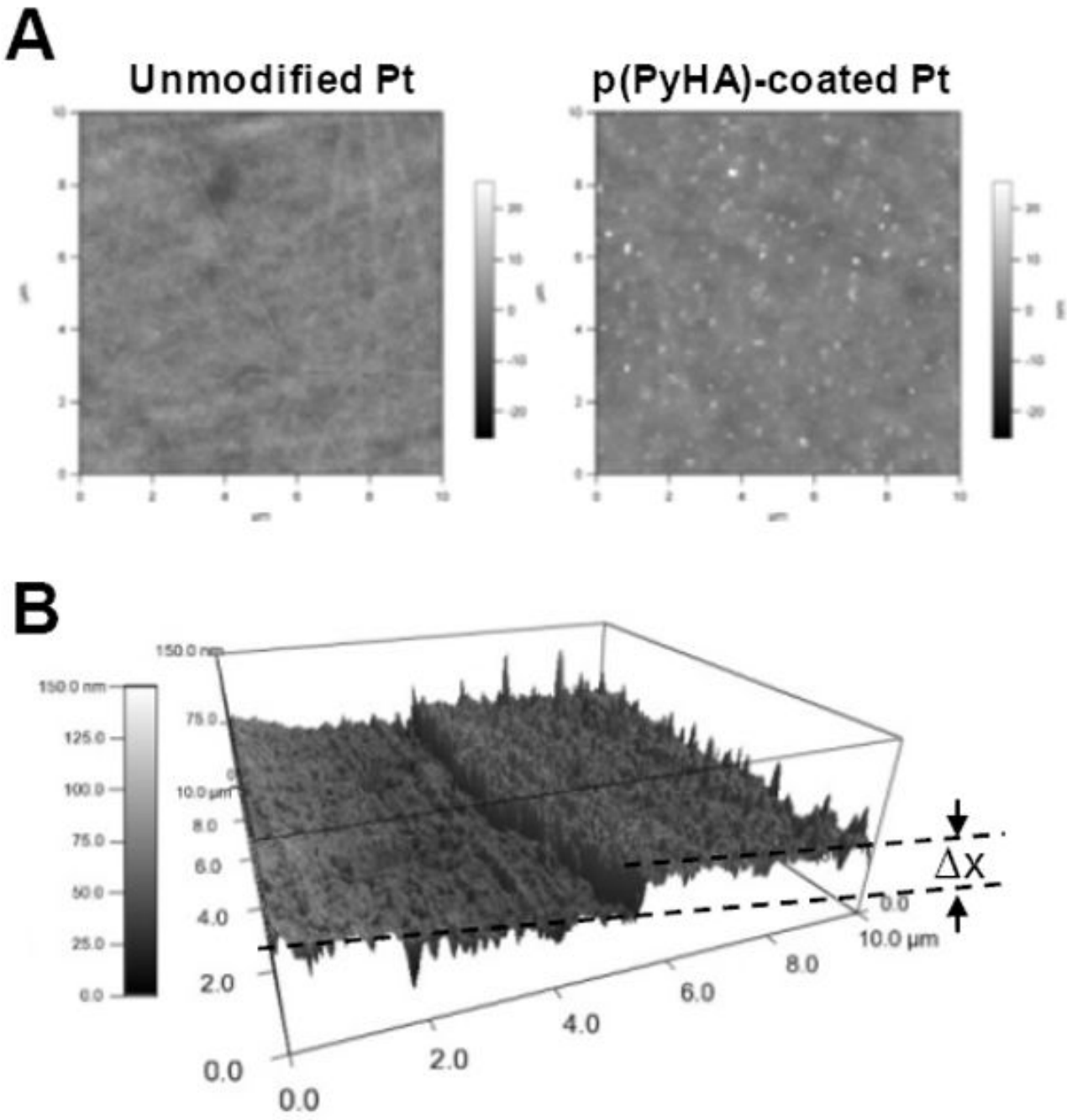

Figure 4.
(A) AFM images of bare Pt and HA-coated Pt substrates. The p(PyHA) coating of Pt decreased surface RMS roughness, but formed nano-clusters on the surfaces. (B) The border between bare Pt and the HA-coated area was scanned, indicating a thickness (Δx) of 20-40 nm thickness for dry films.

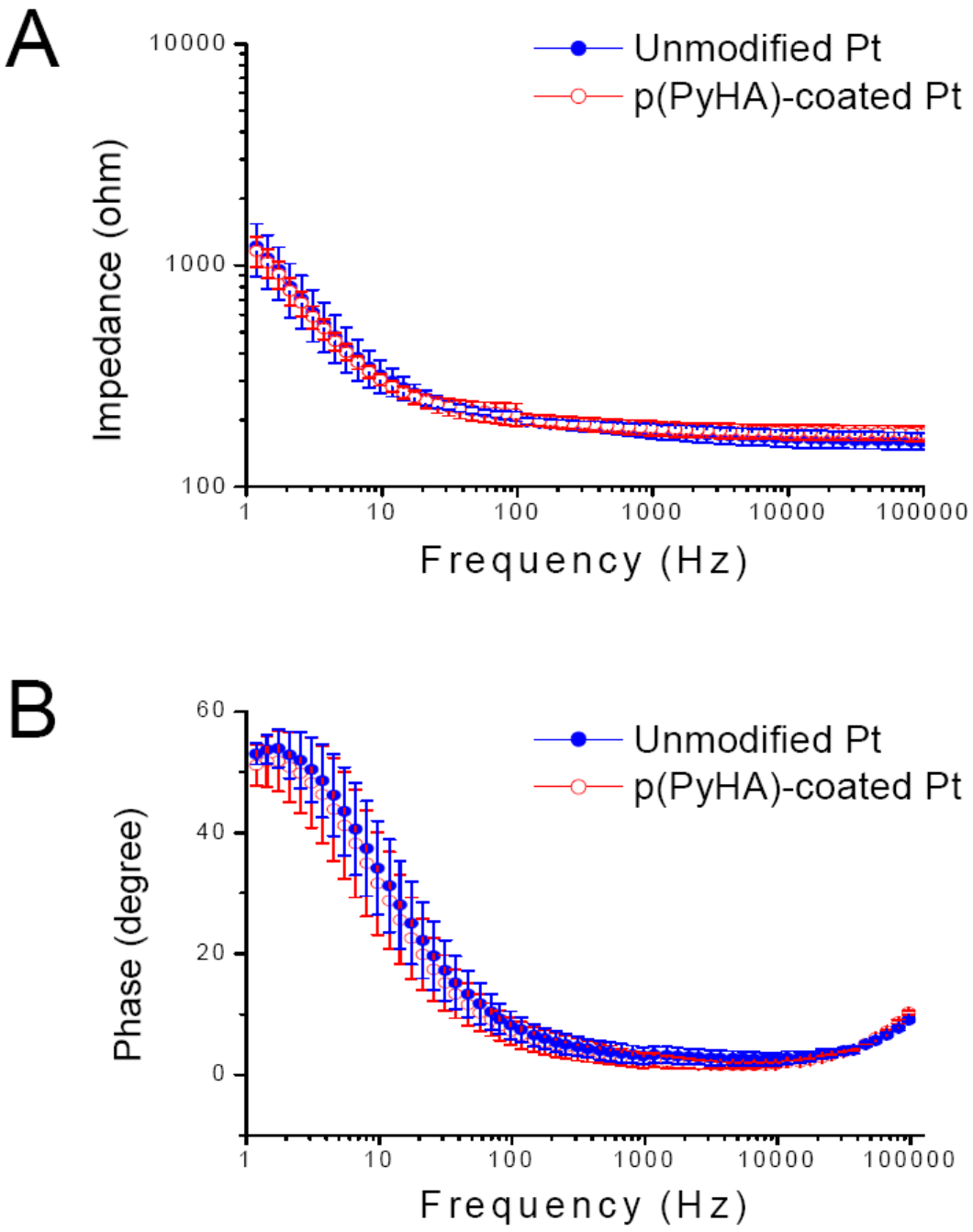

Figure 5.
(A) Magnitudes and (B) phase angles of impedance for unmodified Pt and p(PyHA)-coated Pt. Impedance spectra were collected in a range of 1-10^5 Hz, applying an AC sinusoidal signal with 10 mV, vs SCE, in PBS solution. Averages and standard deviations were obtained from three samples for each condition.

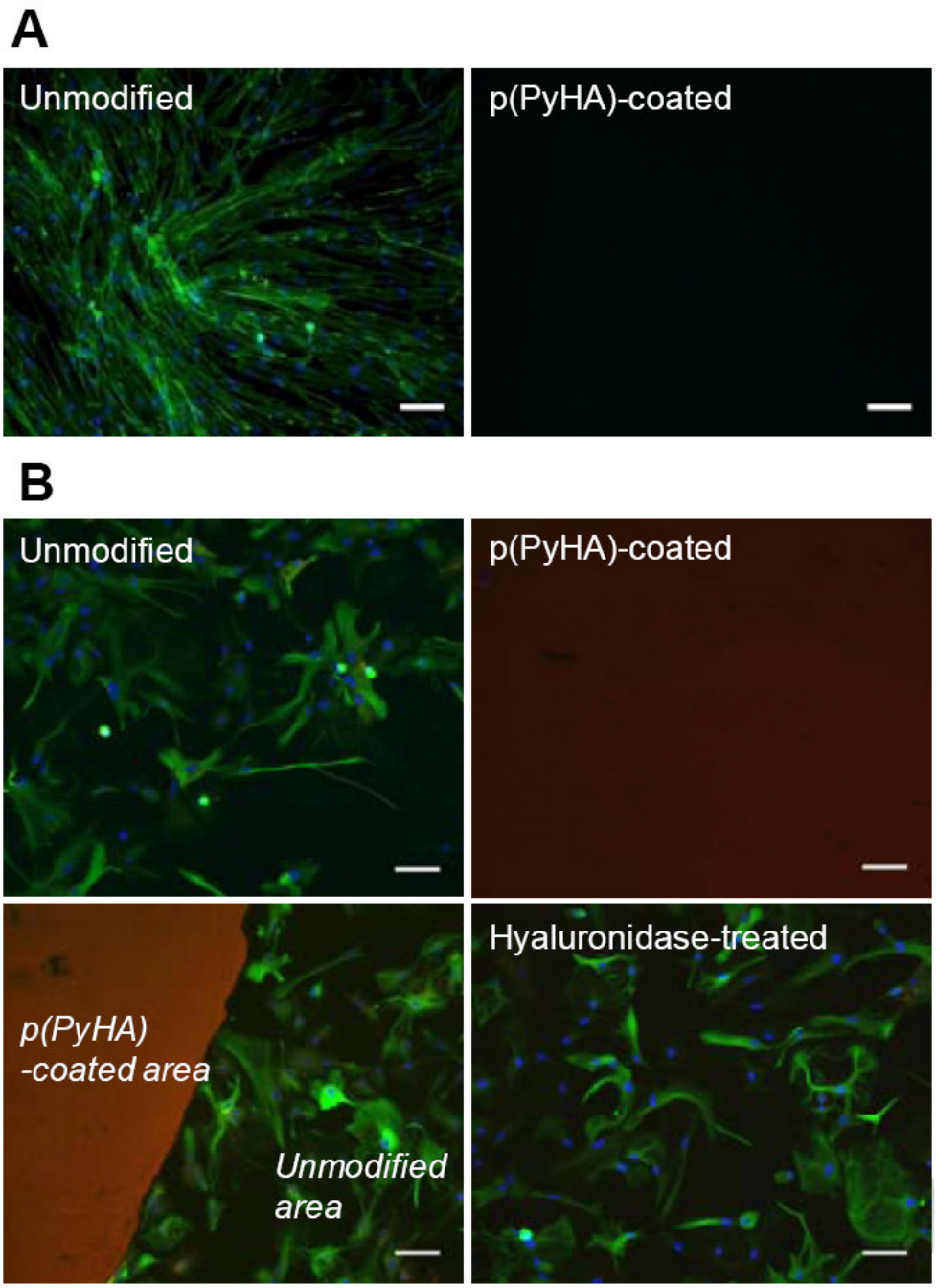

Figure 6.
In vitro cell culture on bare ITO and p(PyHA)-coated ITO. (A) Normal human dermal fibroblast cells (nHDF) were cultured for 3 days and stained for F-actin (green) and nuclei (blue). The nHDF cells did not adhere to the p(PyHA)-coated substrates. (B) Cortical astrocytes were also cultured for 3 days on ITO, p(PyHA)-coated ITO, and HAase-treated p(PyHA)-coated ITO, followed by immunostaining for GFAP (green, astrocyte marker), nuclei (blue), and HA (red). Astrocytes did not grow on p(PyHA)-coated surfaces; however, removal of surface p(PyHA) with HAase permitted adhesion and growth comparable to bare electrodes. Scale bars are 50 μm.

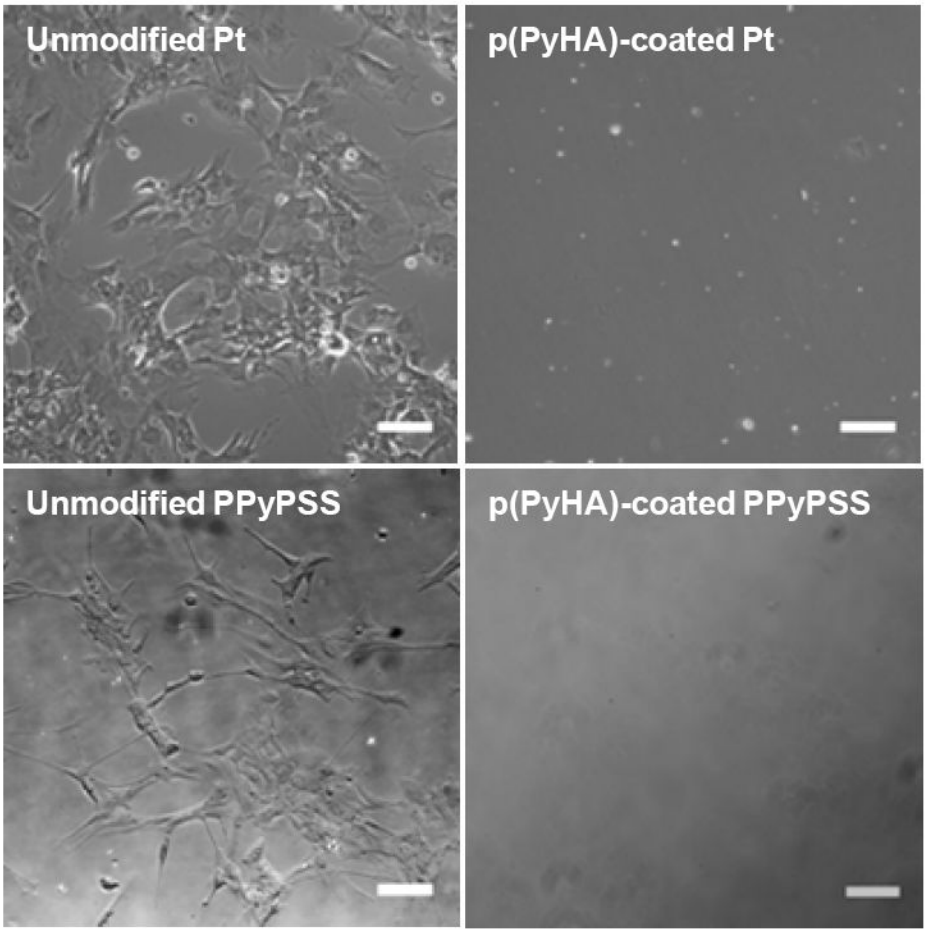

Figure 7.
Phase contrast images of astrocytes cultured on Pt and PPyPSS substrates either unmodified or coated with p(PyHA). Astrocytes did not grow on surfaces with the p(PyHA)-coating, whereas unmodified substrates permitted cell adhesion and growth. Scale bars are 50 μm.

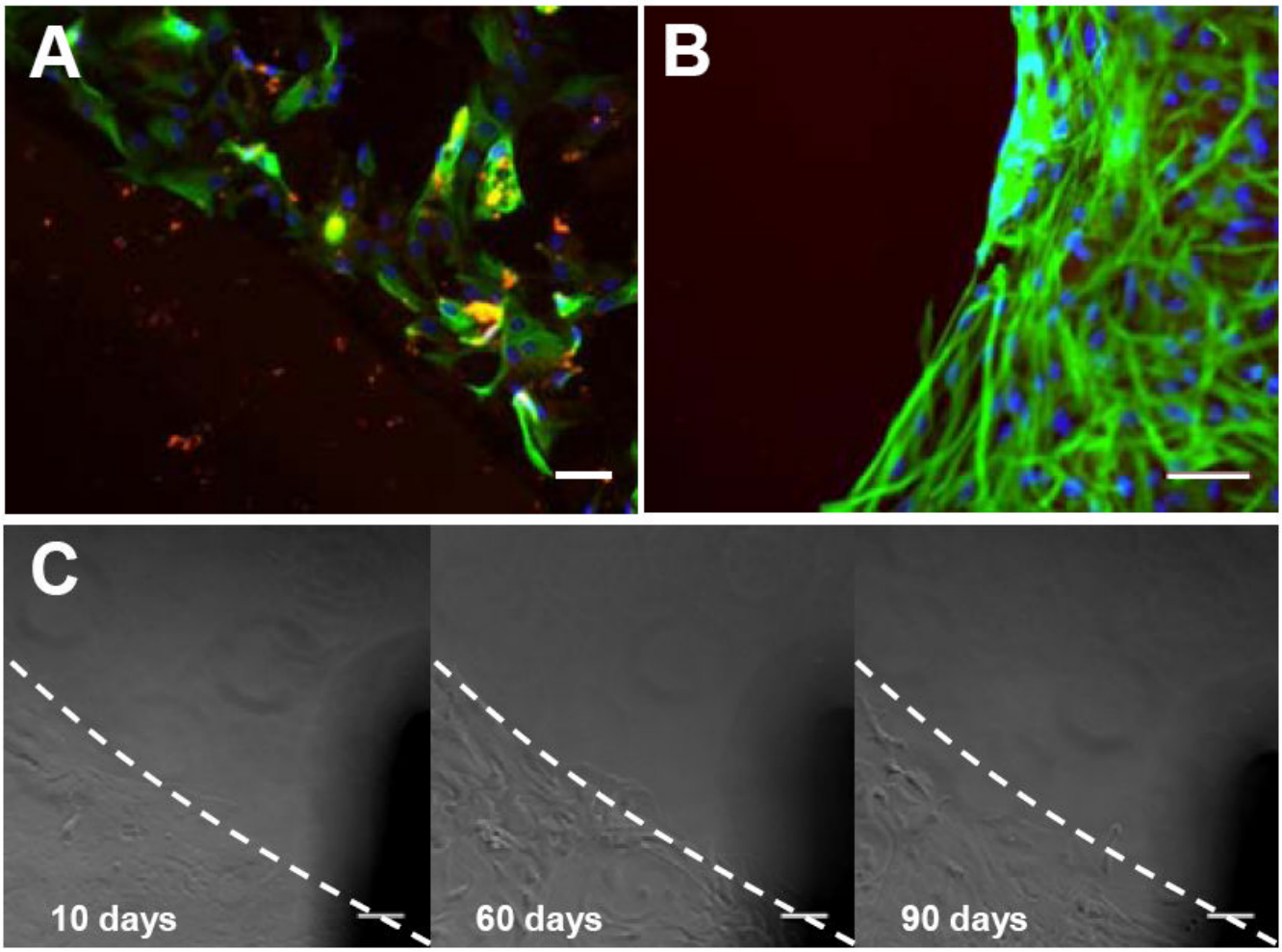

Figure 8.
Functional stability of the p(PyHA) coating. (A) The p(PyHA)-coated ITO was incubated in PBS at 37°C for 3 months, followed by astrocyte culture on the incubated substrates. The dashed line indicates the border between the HA-coated area and the unmodified area. The p (PyHA) coating (red) was stable and resisted adhesion of astrocytes (green for GFAP and blue for nuclei). (B) Long-term astrocyte culture on HA-coated Pt for 1 month. Cells did not attach or migrate to HA-coating during cell culture. (C) Long-term astrocyte culture on HA-patterned ITO for 3 months; images were taken at same location for all time points, showing no adhesion on and migration to the HA-patterned area for 3 months. Scale bars are 50 μm.

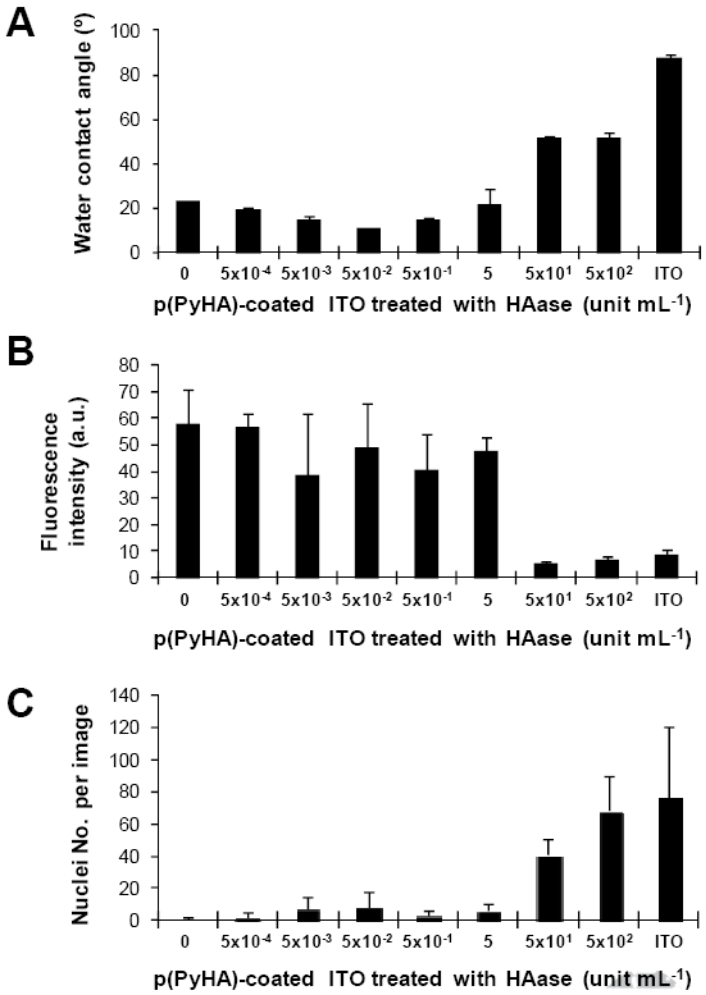

Figure 9.

Enzymatic stability tests of the p(PyHA)-coated ITO. (A) Water contact angles were measured for the HAase-treated substrates (n=3). (B) Immunofluorescence intensities were measured from the HAase-treated substrates (n=3). The HAase-treated substrates were stained with bHABP and streptavidin-PE. All substrates were treated and imaged at the same conditions. (C) Astrocytes were cultured on the HAase-treated p(PyHA) substrates for 3 days and numbers of nuclei were counted (n=5). Averages ± standard deviations are plotted.